

## RESEARCH ARTICLE

# Experimental investigation on emission and combustion characteristics of an industrial burner using biogas co-fired with diesel and biodiesel

Medhat Elkelawy<sup>1</sup>, Ali Kamel Abdel-Rahman<sup>2</sup>, Ahmed Abou-Elyazied<sup>3</sup>, Saad Mostafa El-malla<sup>4\*</sup>

Received: 21 September 2022 / Revised: 30 November / 2022 / Accepted: 6 December 2022 / Published online: 10 December 2022

### Abstract

The purpose of this study is to use biogas produced in industrial wastewater treatment plants to generate energy by co-combustion with diesel fuel or biodiesel to avoid the unstable flow rate of biogas and the variable methane ratio, which determines the biogas energy content. An experimental analysis was conducted in this study to determine the combustion and emissions performance of a 350 KW industrial burner fuelled with three different percentages of biogas: Biogas1 (CH<sub>4</sub> 75%, CO<sub>2</sub> 25%), Biogas2 (CH<sub>4</sub> 70%, CO<sub>2</sub> 30%), and Biogas3 (CH<sub>4</sub> 60%, CO<sub>2</sub> 40%) co-combusted with diesel or waste cooking oil biodiesel. Practical tests have demonstrated that in comparison to biogas and diesel fuel, the CO emission level of co-combustion biogases and biodiesel for B1000Biogas1, B100Biogas2, and B100Biogas3 was reduced by 60%, 50%, and 42%, while NO<sub>x</sub> emission increased by 52%, 47%, and 43%, along with the maximum flame temperature, by 9%, 10%, and 12%, respectively. The flame structures of the fuels in the swirl burner were investigated using flame pictures and contour temperature. The flame color for biodiesel and biogas was more brilliant and intense than for diesel and biogas. All the fuel test results demonstrate that inert CO<sub>2</sub> in biogas composition has a substantial influence on the chemical reactions occurring in the flame and pollutant emissions due to its dilution effect and slowing oxidation reaction. The higher inert CO<sub>2</sub> gas ratio in biogas caused a reduction in reaction intensity, which resulted in a weaker, unstable flame and also decreased flame temperature and NO<sub>x</sub> emissions. yield as well as high fermentation efficiency.

**Keywords:** Biogas; Diesel; Biodiesel; CO<sub>2</sub>; Emission; Temperature.

<sup>1</sup>Mechanical Power Engineering Department, Faculty of Engineering, Tanta University, Egypt.

<sup>2</sup>Mechanical Power Engineering Department, Faculty of Engineering, Assiut University, Egypt.

<sup>3</sup>Horticulture Department, Faculty of Agriculture, Ain Shams University, Egypt.

<sup>4</sup>Faculty of Sugar and Integrated Industries Technology, Assiut University, Egypt.

\*corresponding author: [saad\\_pg1230149@sit.aun.edu.eg](mailto:saad_pg1230149@sit.aun.edu.eg)

### Introduction

Due to the current global energy crisis and climate challenges brought on by fossil fuel emissions, there has recently been an increase in the demand for biofuels to replace conventional fuels such as biogas and biodiesel. Biogas is one of the most important types of biofuels and has several advantages, like being a renewable and ecologically benign fuel that can be used in internal combustion engines and boilers with little or no modification because of its similar composition to natural gas (KIPYEGON 2011). Biogas is anticipated to be able to supply 25% of the target consumption of renewable energy in the future Miltner et al. (2017). Sugar beet factories consume a lot of energy. Therefore, finding inexpensive alternatives is necessary to reduce the amount of steam consumed and maximize the financial benefit of these alternatives. One of these solutions is to use the enormous amounts of biogas produced in industrial wastewater treatment facilities.

The biogas produced in biogas facilities by the anaerobic digestion of bacteria consists primarily of a variable ratio of methane, ranging from 50 to 80 percent. The second major component of biogas is carbon dioxide, which is present in varying proportions ranging from 50% to 20%, as well as a minor amount of other gases and trace elements. The metabolic process known as anaerobic digestion occurs in a reductive environment without the presence of an oxygen source Divya et al. (2015). Anaerobic digestion has been extensively employed for the disposal of easily biodegradable organic waste.

Microorganisms break down the organic carbon (biomass) into a more manageable substance, and the result is a gas primarily made of methane and carbon dioxide. According to De Mes et al. (2003); Weiland (2010), there are four main steps in anaerobic digestion. Each one involves a complex microbiological procedure and a string of metabolic reactions. Hydrolysis is the initial process. The simple soluble organic molecules, such as sugars and amino acids, are produced during the hydrolysis of the complex organic matter with long hydrocarbons, such as polysaccharides and proteins. The exo-enzymes of the fermentation microorganisms carry out this activity.

The product of the hydrolysis is fermented in the second process, known as acidogenesis, where it is converted into volatile acids, hydrogen, carbon dioxide, and a negligible amount of ethanol, other alcohols, and lactate. Acetogenesis is the third stage. The acetogenic bacteria transform the fermentation product into acetate, hydrogen, and carbon dioxide. Methanogenesis, or the production of methane from acetate, hydrogen, and carbon dioxide, is the fourth phase. Liu et al. (2006). Biogas produced in anaerobic digestors might contain up to 80% methane by volume, and its quality would be determined by its source. Balat and Balat (2009). The treatment of a wide range of industrial wastewater with anaerobic digestion technology is increasingly commonplace. In most waste industrial treatment facilities, the collected biogas is flared at the site. Although biogas has many advantages and a promising future in terms of energy conservation and air pollution reduction. Biogas has a lower heating value (around 21.5 MJ/m<sup>3</sup>) than natural gas (about 36 MJ/m<sup>3</sup>) (Hosseini and Abdul Wahid 2015). However, on average, its total chemical energy is adequate to power commercial combustors used to generate electricity and heat (Lee and Hwang 2007). The presence of CO<sub>2</sub> in biogas results in lower flame temperatures and burning rates, as well as a limited range of flame stability, affecting combustion efficiency. Kumar Yadav et al. (2019). Biodiesel is one of the most important alternative biofuels for replacing conventional diesel fuels in industrial burners and diesel engines because it almost matches the properties of diesel Raju et al. (2020) Elkelawy et al. (2022b). Biodiesel is a monoalkyl ester of long-chain fatty acids derived from renewable agricultural resources such as edible and non-edible vegetable oils, animal fat, and waste cooking oils Elkelawy et al. (2020). Vegetable oils are composed of triglycerides, which are tri-esters consisting of three long hydrocarbon chains (fatty acid molecules) (Zhang et al. 2003). By treating these compounds through trans esterification, Triglycerides are degraded into smaller alkyl esters (Moreno Ovalle 2017). The traditional method for producing biodiesel is trans esterification with alkali catalysts. Swamy et al. (2019). In the trans esterification process, the original molecular structure of triglycerides is changed to produce biodiesel and glycerol by reacting triglycerides with an alcohol (such as ethanol or methanol) in the presence of a catalyst (such as sodium hydroxide) at an elevated temperature (Love 2009).

The goal of the conversion trans esterification process is to reduce the viscosity of the oil (Alagu et al. 2019), and in this process, the fatty acids of vegetable oil exchange are placed with the (OH) groups of the alcohol-producing glycerol and methyl, ethyl, or butyl ester depending on the type of alcohol used (Venu et al. 2019a). One of the main obstacles to the commercialization of the production of biodiesel from vegetable oils is the high cost of production, which is caused by the high cost of virgin vegetable oil. Cooking oil waste is a key component in the up to 60–90% price reduction of biodiesel production Talebian-Kiakalaieh et al. (2013). Several studies have been conducted to enhance the yield of biodiesel from waste cooking oil by optimizing the

traditional alkali-catalyzed trans esterification reaction factors Elkelawy et al. (2019).

The molar ratio, the type and quantity of catalyst, the reaction time and temperature, and the amount of free fatty acids (FFAs) are the main parameters influencing the alkali-catalyzed transesterification reaction and biodiesel yield Rashid et al. (2008). Meng et al (2008) investigated experimentally and analytically to determine the optimum conditions of the trans esterification reaction of Biodiesel production from waste cooking oil WCO. The result shows that the orthogonal test's optimum experimental conditions were a 9:1 methanol/oil molar ratio, 1.0 weight percent sodium hydroxide, 50 °C, and 90 minutes.

Experiments test showed that a 6:1 methanol to oil molar ratio was more favorable for the process, and at that ratio, WCO conversion efficiency achieved 89.8%. Phan and Phan (2008) investigated the effects of methanol/waste cooking oils ratio, potassium hydroxide concentration, and temperature on the biodiesel conversion from waste cooking oil WCO.

The result shows that a Biodiesel yield of 88–90% was obtained at the methanol/oil ratios of 7:1–8:1, temperatures of 30–50°C, and 0.75 wt% KOH. Issariyakul et al. (2007) yielded up to 97% ethyl ester from waste cooking oil using a two-stage trans esterification process that was acid and alkali catalyzed. (Leung and Guo 2006) produced biodiesel from the conversion of waste cooking oil using alkaline-catalyzed trans esterification, and the maximum biodiesel yield is approximately 86%. In an industrial burner, biodiesel can be used pure or blended without any modifications. However, the physical and chemical differences between biodiesel (a mixture of saturated and unsaturated long-chain fatty acid mono-alkyl esters) and normal diesel fuels (a mixture of paraffinic, naphthenic, and aromatic hydrocarbons). Raju et al. (2020) affect burner performance and pollutant emissions.

The result showed that the dual-fuel PME/NG flame structure is similar to the single-fuel PME. When compared to diesel at the same equivalency ratio, PME and PME/NG flames emit higher peak intensities of OH\* and CH\* radicals. When compared to pure diesel and PME spray flames, PME/NG dual-fuel produced lower emissions performance because stratification of the fuel/air mixture increases inhomogeneous mixing and results in high CO and NO emissions. On the other hand, Comparing the flame emissions at  $\Phi = 0.65$  and  $\Phi = 0.9$  reveals that the former produced comparable CO but higher NO than single-fuel flames, and the latter produced comparable NO but high CO. This is caused by the flame temperature, the amount of flow field turbulence, and the presence of an oxidizer. The co-combustion of crude glycerin with natural gas (NG) and hydrogen in a laboratory furnace burned by a swirl burner was studied by Queirós et al. (2013) for combustion and pollutant emission.

With the use of an air-assist atomizer, the glycerol is sprayed into the combustion chamber. To create a combustible mixture that could be burned, the fuel vapor was mixed with natural gas and hydrogen. The findings revealed that whereas neat natural gas emissions are often higher, NO<sub>x</sub> emissions from the combustion of glycerol, natural gas, and hydrogen are generally lower. The CO and HC emissions decreased substantially as the AFR rose to 1.5; after that point, they started to rise and were always higher than the emissions from neat natural gas. and also Deposits of Na, K, and Cl, quickly generated near the burner outlet and on the furnace walls during the co-combustion of large amounts of glycerin with gaseous fuels which can threaten long-term furnace use in these conditions. Sidey and Mastorakos (2017) studied experimentally and numerically the effect of the co-combustion of alcohol C<sub>2</sub>H<sub>5</sub>OH and methane CH<sub>4</sub> on Flame structure and stabilization. Ethanol is sprayed at the center of the burner Using a pressure atomizer, and methane is premixed with air. they found that Photographs and mean OH chemiluminescence images indicate that adding CH<sub>4</sub> to a C<sub>2</sub>H<sub>5</sub>OH spray flame broadens the reaction zone and alters its stabilization behavior and the air/fuel range of a stable flame decrease as the amount of gaseous fuel CH<sub>4</sub> rises, and the chances of lifting the flame rise. Sidey and Mastorakos (2018) continued their investigation using the same burner design, experiment, and measurement strategy. However, they substituted C<sub>7</sub>H<sub>16</sub> with ethanol. Flame imaging demonstrates that the stabilization characteristics of one fuel, whether liquid or premixed gaseous, are impacted by the presence of additional fuel.

The result shows that the presence of the second fuel may destabilize the typical attachment points characteristic of the first fuel. However, dual-fuel spray flames are more resistant to blow-off than single-fuel spray flames. Adam et al. (2022) investigated the combustion performance of cofiring diesel with LPG in the burner. All the tested conditions are conducted at the same thermal power of 70 kW and equivalence ratio of 0.5.

The findings indicated that cofiring dual fuels raises the temperature inside the furnace, improving convective heat transfer and shortening the lengths of the thermal and visual flames. The efficiency is also increased by cofiring. Zhen et al. (2013) experimentally investigated the effect of hydrogen addition on the characteristics of the biogas flame and combustion. They found that the addition of hydrogen significantly improves the stability of the biogas flame and combustion properties.

As increase hydrogen addition rates, the flame temperature increases, and the length of the visible flame decreases. Leung and Wierzbza (2008) have carried out an experimental study of the flame stability behavior of biogas mixtures of varying composition as a function of co-flowing stream velocity and the effect of hydrogen addition on the flame stability of such fuel mixtures. Finding that the significant decrease in the stability limits of biogas diffusion flame due to the presence of a large amount of CO<sub>2</sub> can be improved through the addition of a small amount of hydrogen into the biogas.

**Table 1.** Summarizes the main results of studies on biogas co-firing with hydrocarbon fuels.

Author	Type of fuels	Results
(Kurji et al. 2017)	CO <sub>2</sub> /CH <sub>4</sub> , diesel, biodiesel	At CO <sub>2</sub> increase in the mixture, CO increases. NO <sub>x</sub> and flame temperature decrease.
(Jiang 2014)	Methane, glycerol	low No <sub>x</sub> and CO emissions.
(Agwu and Valera-Medina 2020)	diesel, synthetic gas	as the syngas percentage in the fuel mix rises, The flame stability rose, No <sub>x</sub> decreased, and CO emissions increased
(Agwu et al. 2020)	waste cooking oil biodiesel, methane	As the methane ratio rises. No <sub>x</sub> levels have dropped. Unburned hydrocarbon increased, combustion efficiency decreased, and flame wrinkling increased
(Altaher et al. 2012)	biodiesel, natural gas, kerosene	No <sub>x</sub> emissions, UHC, and CO emissions decreased.
(Chong et al. 2020)	Biodiesel methyl-esters (PME), natural gas	-high CO and NO emissions. -lower CH* and OH* radical intensities as compared to the neat PME fuel
(Queirós et al. 2013)	natural gas, hydrogen, glycerol	As AFR rises, CO decreases until 1.5, after which they rise. And No <sub>x</sub> increase
(Sidey and Mastorakos 2017)	Alcohol C <sub>2</sub> H <sub>5</sub> OH, methane CH <sub>4</sub>	As the CH <sub>4</sub> increases, the probability of flame lift-off increases
( Adam et al. 2022)	diesel, LPG	Cofiring dual fuels improve efficiency, increases soot oxidization, raises furnace temperature, and shortens thermal flame lengths.
(Zhen et al. 2013)	Biogas.Hydrogen	the flame temperature increases and the length of the visible flame decreases.

In light of the energy crisis, one of the critical issues that must be addressed is the use of available and inexhaustible alternative fuels such as biogas and biodiesel in the industrial sector. The current experiments demonstrate the feasibility of co-combustion biofuels such as biogas and biodiesel without modifying the industrial burner, and the results show the possibility of industrial application of two types of biofuels, as exhausts are reduced and combustion efficiency is increased when compared to diesel.

The current study aims to determine the effect of the co-firing of three ratios of biogas with diesel or biodiesel on the combustion and pollutant emission characteristics of industrial oil burners installed in boilers or furnaces. Three ratios of biogas and a constant flow rate of diesel or biodiesel were used in the experiment, with the equivalent ratios of 0.5, 0.7, 1, and 1.6. The presented data shows CO and NO<sub>x</sub> emissions as well as temperature to identify the combustion characteristics within the flame zones.

### Experimental test setup

An arrangement diagram is shown in Figures 1 and 2. A multi-biofuel industrial burner is designed and constructed in a laboratory-scale furnace to analyze chemical reactions and examine the combustion system's flow, flame, and exhaust. A swirl atomizer-type diesel oil fuel burner (CUENOD, France Manufacturing) with a maximum heat capacity of 350 KW was used for all experiments, which were carried out in a horizontal steel test chamber coated on the inside with refractory bricks. The experiment's burner was placed inside the chamber at the beginning and center of the furnace. The furnace measured 1500 mm in length and 500 mm in diameter. The chamber's wall had a moveable window measuring 96 cm by 25 cm to provide optical access and four measuring holes with a diameter of 2.5 cm each to facilitate thermocouple temperature measurement. From the burner's inlet, they were spaced 0, 0.3, 0.6, and 0.9 meters apart. A chimney was also installed at the end of the furnace, measuring 2500 mm in length and 12.7 mm in diameter, to suck and exhale the combustion products. The combustion air supply system consists of a burner blower, three independent blowers, an air intake pipe, and an orifice meter for airflow measurement. The air blower's flow rate is regulated by valves and an on/off electronic control panel, and the fuel was fed by gravity from the tank above the burner and a fuel pump that is operated by the burner's motor. The fuel flow rate was maintained constant at 0.12 liters per minute while the airflow rate was changed to create five different equivalent ratios. The premixed gas and liquid flows were passed separately. Methane and carbon dioxide are mixed in the mixture pipe in the specified ratios. They are introduced into the burner's gas line, and the fuel-air mixture passes through a swirled with axial curved vanes at a 30-degree angle

before being mixed with liquid fuel and combustion together. The flame temperature profiles were measured using an R-type thermocouple with a wire diameter of 0.12 mm, a bead diameter of 6 mm, and a length of 70 cm. Four thermocouples were positioned on a multi-dimensional linear traversing mechanism. In addition, the temperature of the exhaust was measured using an R-type thermocouple that was put in the exhaust pipe. A controller was used to gather temperature data. This thermocouple was set up throughout the length of the flame using a guided traverse mechanism. Temperature profiles were gathered in the flame at various axial and radial positions. The concentration of exhaust gases CO and NO<sub>x</sub> can be measured using the Garboard—5020 emission gas analyzer. Measurements were made on the emissions levels and combustion efficiency of combination fuels.

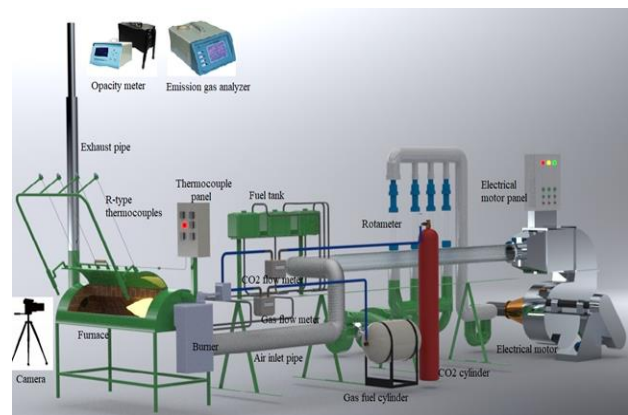


Figure 1. a schematic diagram of the test rig.



Figure 2. Direct photo of the testing apparatus in the laboratory

### Analysis of Experimental Uncertainty.

To ensure that the results were accurate, an uncertainty analysis was done. many factors influence uncertainties. The two most important variables are equipment accuracy and experiment reproducibility. Data on the experimental value range and instrument precision are included in Tables 2 and 3. The root-sum-squared (RSS) method was used in this study to determine the uncertainty of the independent variables of the errors associated with the measured parameters

Moffat (1988).

Equations 1 and 2 are used to compute the mean value and standard deviation of the data Chen et al. (2012) Ratel et al. (2015).

$$\bar{X} = \frac{1}{n} \sum_{i=1}^n X_i \tag{1}$$

$$\sigma_i = \left[ \frac{1}{n-1} \sum_{i=1}^n (X_i - \bar{X})^2 \right]^{\frac{1}{2}} \tag{2}$$

mean value of output measured data, n number of the repeatability of the experiment for measured data (dimensionless). X measured output data. is the standard deviation of measured data. The uncertainty of the measured variable (Wx) as a result of the experiment repeatability for parameter X is calculated as shown in equation 3.

$$W_{x_n} = \frac{\sigma}{\sqrt{n}} \tag{3}$$

The total uncertainty (WR) of various physical quantities measured by the sensors and instruments was calculated using equation 4. Pourhoseini et al. (2021).

$$w_r = \left[ \left( \frac{\partial R}{\partial x_1} W_{x_1} \right)^2 + \left( \frac{\partial R}{\partial x_2} W_{x_2} \right)^2 + \dots + \left( \frac{\partial R}{\partial x_n} W_{x_n} \right)^2 \right]^{1/2} \tag{4}$$

Where R is a function of X, WR represents the dependent variable total of uncertainty. X1 and Xn are the independent variables of measured data. Wx1, Wx2, and Wxn are the uncertainties of the independent variables.

**Table 2.** Specification of measurement equipment.

Specifications of Gasboard-5020 gas analyzer			
	Range	Accuracy	Resolution
CO	0-10%	Rel ±3% Abs ±0.06%	0.01%
NOx	0-5000 ppm	Rel ±5% Abs±25 ppm	1 ppm
Specifications of R-type thermocouple			
R-type thermocouple	0-1600 C°	0.25%	1.5 C°
Specifications of Rotameter			
Air flow sensors	18-180 m3/hr.	±6%	

**Table 3.** Specification of liquid fuel meter type aquametro VZO 8.

Type	liquid fuel meter type aquametro VZO 8	
Maximum Flow Rate Qmax	l/h	200
Nominal Flow Rate Qn	l/h	180
Minimal Flow Rate Qmin	l/h	4
Approx. Starting Flow Rate	l/h	1.6
Maximum Permissible Error	±1% of Actual Value	
Repeatability	±0.2%	
Smallest Readable Amount:	l	0.01
Registration Capacity	m <sup>3</sup>	1 000

**Experimental fuel.**

**Waste cooking oil biodiesel (WCO) production and properties.**

Biodiesel is produced from waste cooking oil by the alkaline transesterification process. Two processes make up the WCO biodiesel production process, as shown in figure 3: the first includes reaction, and the second involves washing. the first step in the production of WCO biodiesel from waste oil involved the esterification process using 1% alkaline catalyst (NaOH) on a mass basis of the crude oil (Kumaran et al. 2014). Methanol was used with the crude oil at a molar ratio of 6:1, and the alkaline catalyst (NaOH) was pre-mixed with methanol by a mechanical stirrer to create sodium methoxide and water then the mixture was added with the waste cooking oil and stirred at 600 rpm (Venu et al. 2019b). Since methanol has a boiling point of 63 °C, the reaction temperature for the transesterification process was adjusted to 65–70 °C to avoid methanol vaporization during the biodiesel synthesis process. The transesterification process reaction took 60 minutes to complete Topare et al. (2022). After the esterification process was completed, the reaction oil was placed into a separator funnel for 12 hours to ensure adequate separation of the biodiesel and glycerol layers due to the difference in their densities. Elkelawy et al. (2020). The second stage of producing biodiesel is the washing stage. washing the biodiesel that has exited the transesterification reactor with water to neutralize the catalyst and convert any remaining soaps into free fatty acids. Balat (2007). Pinto (2012). To separate water and dirt from biodiesel, hot water is used at 100 °C in a volumetric ratio of 1:1 for one minute under suitable mixing conditions. This process is repeated approximately 3:5 times until clean water is obtained after washing. During the washing stage, biodiesel's color, which became cleaner and density decreased Elkelawy et al. (2022b).

The process of drying the washed methyl ester product to lower the water content to an acceptable level for biodiesel required standards.

As shown in equation 5, product yield is defined as the weight percentage of the finished product (biodiesel) relative to the weight of waste cooking oil.

Product yield = weight of waste cooking oil/weight of the final product (biodiesel) (5)

In lab experiments, the highest biodiesel production of 90% was achieved at a volumetric methanol-to-oil ratio of 0.25:1 and a weight catalyst concentration of 1%. The parameters of diesel and biodiesel characteristics of the tested fuels were measured at the National Research Center (NRC-Dokki) in Egypt in line with ASTM standards, as shown in Table 4.

The diesel fuel used in the experiments was obtained locally from a commercial petroleum source. Raw waste cooking oil was obtained from homes and restaurants to produce biodiesel in a lab.

**Table 4.** The properties of diesel D100 and Biodiesel B100.

Experiment	Test method	Standard Limits	Diesel D100	Biodiesel B100
Density @ 15.56°C g/cm <sup>3</sup>	ASTM D-4052	0.86–0.9	0.8370	0.9064
Kinematic viscosity, CST @ 40° C mm <sup>2</sup> /s	ASTM D-445	1.9 – 6.0	4.38	7.17
Total sulfur, wt %	ASTM D-4294	Max 3%	0.231	Nil
Total acid number, mg KOH/g	ASTM D-664	MAX 0.50	0.056	0.807
Pour point, °C	ASTM D-97	-15 to -16	0	3
Ash content, wt. %	ASTM D-482	0.010 - 0.180	Nil	Nil
Cetane index	ASTM 4737	Min 40	0	46
Copper corrosion	ASTM D-130	No.3 Max	1a	1a
Calorific value KJ / Kg	ASTM D-240	Report	44547	37523

Separatory funnel of the first stage of the esterification process.

Separatory funnel of the second stage of the washing of the biodiesel.



**Figure 3.** photo of the first and second stages of biodiesel production.

## Results and Discussion

For laboratory testing, biodiesel derived from waste cooking oil and diesel fuel is prepared. Diesel fuel is used to operate the furnace at first, and it burns continuously at a rate of 0.12 liters per minute. The air is then forced to push the methane and carbon dioxide mixture, and three different ratios of biogas—Biogas1 (CH<sub>4</sub> 75%, CO<sub>2</sub> 25%), Biogas2 (CH<sub>4</sub> 70%, CO<sub>2</sub> 30%), and Biogas3 (CH<sub>4</sub> 60%, CO<sub>2</sub> 40%) are co-combusted with diesel fuel.

The experiments are repeated using biodiesel instead of diesel fuel. Combustion and exhaust emissions are studied for each ratio of biogas and diesel or biodiesel at four different equivalent ratios of 0.5, 0.7, 1, and 1.6.

The number of samples for all experiments is six since three ratios of biogas are co-combusted with diesel or biodiesel, as shown in Table 5.

**Table 5.** The types of fuels used in the experiment.

NO	Types of fuels	Description
1	D100biogas1	100% diesel, CH <sub>4</sub> 75% and CO <sub>2</sub> 25%
2	D100biogas2	100% diesel, CH <sub>4</sub> 70% and CO <sub>2</sub> 30%
3	D100biogas3	100% diesel, CH <sub>4</sub> 60% and CO <sub>2</sub> 40%
4	B100biogas1	100% biodiesel, CH <sub>4</sub> 75% and CO <sub>2</sub> 25%
5	B100biogas2	100% biodiesel, CH <sub>4</sub> 70% and CO <sub>2</sub> 30%
6	B100biogas3	100% biodiesel, CH <sub>4</sub> 60% and CO <sub>2</sub> 40%

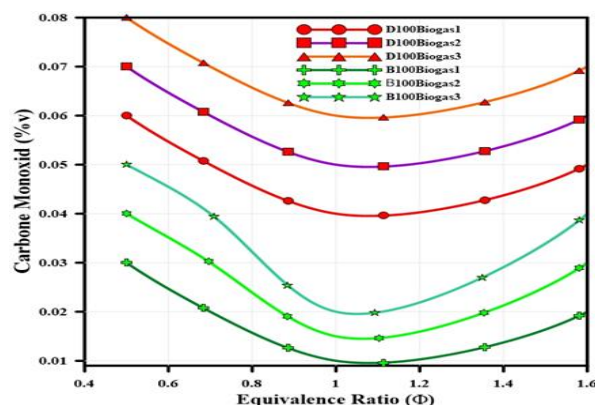
### Carbone monoxide CO emission characteristics

Figure 4 shows the trend lines of CO emission fluctuations with different equivalence ratios for the co-combustion of biogas with diesel or biodiesel. In all cases, the equivalence ratio and different types of fuels have an impact on CO emission levels.

It is clear from Figure 4 that CO emission increases in the lean mixture region and falls at the equivalence ratio of 1.0 ( $\Phi = 1$ ) under stoichiometric conditions, then increases in the rich fuel region due to excessive fuel consumption and insufficient air supply, which promote higher CO production during combustion. All the fuel types follow the same trend.

Biogas and biodiesel fuel co-combustion emit less carbon monoxide than diesel and biogas. CO emissions decreased by about 60%, 50%, and 42% for B100biogas1, B100biogas2, and B100biogas3, respectively, compared to the co-combustion of biogas and diesel. Figure 4 shows that biodiesel, when burned with biogas, enhances the combustion process and accelerates the conversion of carbon monoxide to carbon dioxide, resulting in an improvement in oxidation stability and complete combustion compared to diesel. due to biodiesel containing a sufficient amount of oxygen Mahfouz et al. (2017). However, in the case of co-combustion of biogas with biodiesel, the level of carbon monoxide emissions increases as the inert carbon dioxide content in biogas rises.

In general, the level of carbon monoxide emissions is significantly affected by any change in the percentage of carbon dioxide content in the biogas composition. As the percentage of carbon dioxide in the biogas increases, the carbon monoxide emissions resulting from combustion increase the result of the high concentration of the inert dilution gas  $\text{CO}_2$ , which lowers the flame temperature and impacts on the rate of the reaction that forms carbon monoxide and produces more carbon monoxide emissions. Zhang et al. (2019). As shown in Figure 4, the low content of inert gas  $\text{CO}_2$  in the biogas compositions for B100biogas1 and D100biogas1 reduces carbon monoxide emissions and tends to bring the combustion closer to being complete.



**Figure 4.** The trend lines of CO variation with an equivalent ratio.

### Nitrogen Oxide NOx

NOx refers to nitrous oxide, nitric oxide, and nitrogen dioxide in the combustion system. The temperature inside the furnace, the amount of oxygen present, the amount of time needed for the reaction to take place, the equivalency ratio, and the composition of fuels all have a substantial impact on NOx production. Figure 5 depicts the differences in NOx emissions as they relate to various fuels and equivalence ratios.

The highest amount of NOx emissions from all fuels were measured at a high equivalence ratio of 1.6 ( $\Phi = 1.6$ ), due to the high flame temperature. With a low equivalence ratio, NOx decreases, resulting in lower flame temperatures, which inhibit the production of thermal NOx. Bazooyar et al. (2015).

Figure 5 demonstrates that the co-combustion of biodiesel and biogas emits higher nitrogen oxide emissions compared to conventional diesel.

This is because the composition of biodiesel contains double bonds, which enhance the flame temperature and accelerate the creation of NOx by the thermal (Zeldovich) NOx mechanism. Additionally, the substantial amount of oxygen included in biodiesel enhanced the combustion process and led to complete combustion Subramani and Venu (2019), which further increased the flame temperature and increased NOx emissions. Janakiraman et al. (2020) (Ban-Weiss et al. (2007).

The NOx level emissions of co-combustion biodiesel with biogas (B100biogas1, B100biogas2, and B100biogas3) significantly increased by 52%, 47%, and 43%, respectively, compared to co-combustion diesel with biogas. In all cases and at different equivalency ratios, the trend of NOx emission for different fuels illustrates the significant influence of inert  $\text{CO}_2$  content in biogas. As the proportion of carbon dioxide in the fuel mixture rises, the NOx emission level decrease.

The reductions in NOx emissions for the diesel co-combustion with biogas (D100Biogas2 and D100Biogas3) compared to D100Biogas1 are 19% and 36%, respectively. In addition, the reduction in NOx emissions for the biodiesel co-combustion with biogas (B100Biogas2 and B100Biogas3) compared to B100Biogas1 is 13% significant impact on the fuel mixture as a result of the dilution effect of carbon dioxide and the increased cooling effect, which reduces the rate of CO and  $\text{H}_2$  oxidation reactions and hence the exhaust temperature (Lee et al. 2012).

and 24%, respectively. This result is due to the effect of inert and non-flammable carbon dioxide, which inhibits combustion reactions and consequently lowers the flame temperature, which reduces the amount of nitrogen oxide emissions.

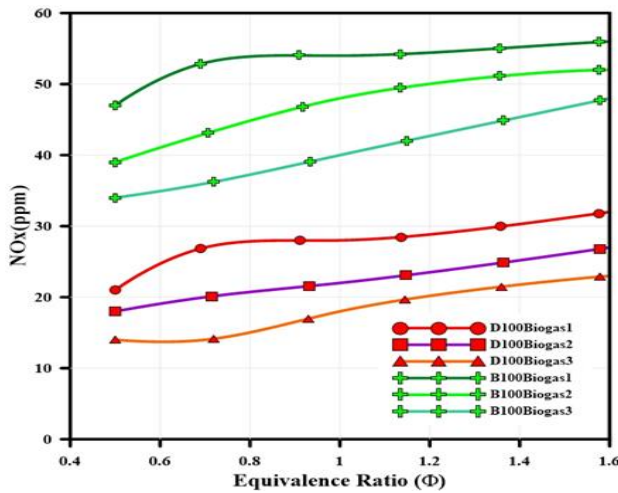


Figure 5. The trend lines of NOx variation with equivalent ratio.

### Combustion performance

#### The effect of different equivalence ratios on the exhaust gas temperature

In general, the combustion temperature rises as the equivalent ratio increases. The R-thermocouple measures the exhaust temperature at the end of the furnace, at a distance of 140 cm from the burner nozzle, and it is clear from figure 6 that all types of fuel increase the exhaust temperature with an increase in the equivalence ratio, as a result of the increased fuel-air mixture, and thus the total combustion temperature increase. This is because the additional fuel in the mixture releases a lot of heat.

Exhaust temperature shows an upward trend with the increase of methane ratio in biogas and its cofired combustion with diesel and biodiesel liquid fuels. But by comparing both fuels, we find that the co-combustion of biodiesel with biogas raises the exhaust temperature compared to diesel, This is because biodiesel contains a higher content of oxygen, which leads to complete combustion and consequently a higher combustion temperature. Venu et al. (2020). The exhaust temperature of co-combustion biodiesel with biogas (B100 Biogas 1, B100 Biogas 2, and B100biogas3) increased by 12%, 9%, and 7%, respectively, compared to co-combustion diesel with biogas. Figure 6 also shows that the exhaust temperature decreases as the amount of inert carbon dioxide gas in the mixture increases. The exhaust temperature decreased when biogas and diesel were co-fired by 2% and 5% for D100biogas2 and D100biogas3, respectively, compared to D100Biogas1, and by 5% and 8% for biodiesel cofiring with biogas for B100biogas2 and B100biogas3,

respectively, compared to B100Biogas1. inert carbon dioxide has a

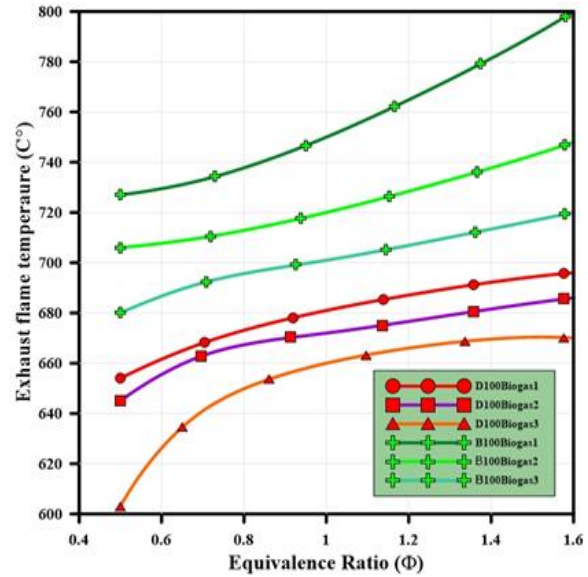


Figure 6. The effect of the equivalent ratio on exhaust gas temperature.

#### The effect of different equivalence ratios on the maximum flame temperature of the combustion chamber

Figure 7 shows the maximum flame temperature for different types of fuels. From the experimental results, the flame maximum temperature increases by increasing the equivalence ratio. The highest maximum temperature was observed at an equivalence ratio of 1.6 for all mixture fuels. This is due to more fuel being burned in fuel-rich mixture conditions. Figure 7 illustrates that the maximum flame temperature decreases as the amount of non-combustible carbon dioxide in the biogas increases Mansour et al. (2020).

This is because the high heat capacity of the CO<sub>2</sub> and its enhanced radiation characteristics allow it to absorb more radiation from the reaction zone, which results in a higher cooling effect. Because of this condition, the furnace's temperature drops. Colorado et al. (2010). Additionally, the dilution impact on combustion reduces the probability of complete combustion, hence the maximum flame temperature during biogas cofiring with diesel or biodiesel is reduced proportionally to the percentage of inert carbon dioxide. In the case of co-firing of biodiesel and biogas with different equivalence ratios, the maximum temperature inside the furnace at the ratios B100Biogas1, B100Biogas2, and 100Biogas3 is higher than that of diesel by 10%,11%, and 12% respectively, due to biodiesel has a high oxygen content, which enhances the combustion rate, contributing to the increased peak temperature in comparison with diesel fuel.



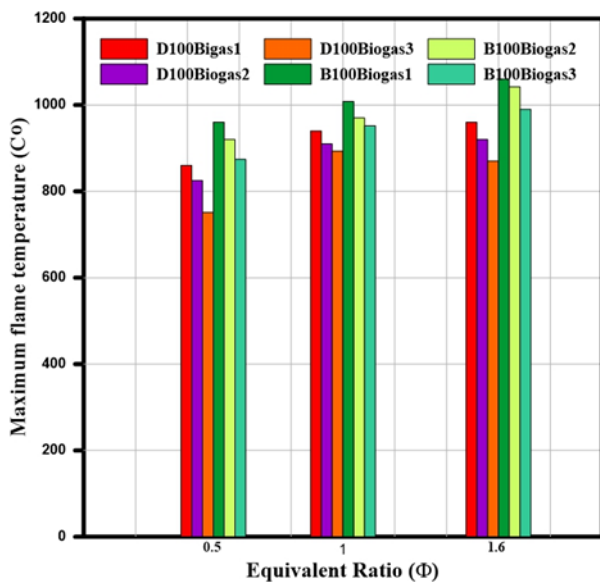


**Figure 7.** The effect of the equivalence ratio on maximum flame temperature.

**The effect of different equivalence ratios on the flame temperature in the centerline of the furnace.**

Flame temperature is the most important characteristic that impacts combustion and pollutant emissions. Four thermocouples were placed along the laboratory furnace to record the temperature difference in the line center of the industrial burner along the furnace during the combustion experiments to understand and compare the flame behavior of different fuels. Figures 8, 9, and 10 demonstrate the differences in flame temperature along the central line of the furnace for various fuel mixtures and different equivalence ratios. From the figures, it can be seen that the gas temperature decreases with a constant trend when the distance from the burner to the end of the furnace increases due to convective and radiative heat transfers. According to the results, the temperature starts to rise from the first thermocouple put at 0 cm from the burner to approximately 30 cm to 40 cm distance from the burner but then starts to fall at 50 cm. This phenomenon occurs because the combustion is most efficient between 30 cm and 40 cm from the burner, which is the hotter zone of the flame. The maximum flame temperature occurs at 30 cm from the burner; this is because complete combustion occurs at this distance, leading to an increase in the average temperature of the flue gas.

The maximum temperature and the trend of temperature distribution from the burner to the end of the furnace decrease as the ratio of inert carbon dioxide present in biogas increases in all fuel mixtures due to the dilution effect of non-combustible carbon dioxide gas, which slows the rate of CO and H<sub>2</sub> oxidation reactions and thus lowers the temperature of the flame inside the furnace. Also, it is noticeable from figures 8, 9, and 10 that the flame temperature along its center line, as measured from the burner to the end

of the furnace, increases in the case of biodiesel co-combustion with biogas compared to diesel for different equivalence ratios. This is because of the effects of the double-bound composition of biodiesel and its high content of oxygen, which raises the temperature of the flame. Additionally, the figures illustrate that the trend of the center line of flame temperature from the burner to the end of the furnace increases as the tested equivalence ratio increases due to more fuel being burned at a higher equivalence ratio for all types of fuel.

Figures 8, 9, and 10 show a comparison of the temperature trends of the burner's center line for three equivalence ratios 0.5, 1, and 1.6. The dual-fuel combustion of biogas and biodiesel or biogas and diesel demonstrate the effect of inert CO<sub>2</sub> on mixture fuels.

In the case of a 0.5 equivalent ratio, as the CO<sub>2</sub> content of biogas increases, the average flame temperature inside the furnace declines by 40 Co and 80 Co, respectively, for B100biogas2 and B100biogas3, compared to B100biogas1, and by 45 Co and 117 Co, respectively, for D100biogas2 and D100biogas3, compared to D100biogas1.

The flame temperature increases as the equivalent ratio increase. For 0.5, 1, and 1.6, the average flame temperature inside the furnace rises by 832 Co, 846 Co, and 930 Co for co-combustion biogas with biodiesel B100biogas1, and by 775 Co, 787 Co, and 815 Co for co-combustion biogas with diesel D100biogas1, respectively. This is due to the addition of an excessive amount of fuel to the mixture, and the co-combustion of biogas with biodiesel is higher than that of diesel because biogas contains a sufficient amount of oxygen than diesel, resulting in higher combustion and a higher average temperature inside the furnace. In addition, the testing results show that biogas with a CO<sub>2</sub> ratio of 40%, B100biogas3, and D100biogas3 significantly reduce the flame temperature in all cases of equivalent ratio when compared to the other types of fuel.

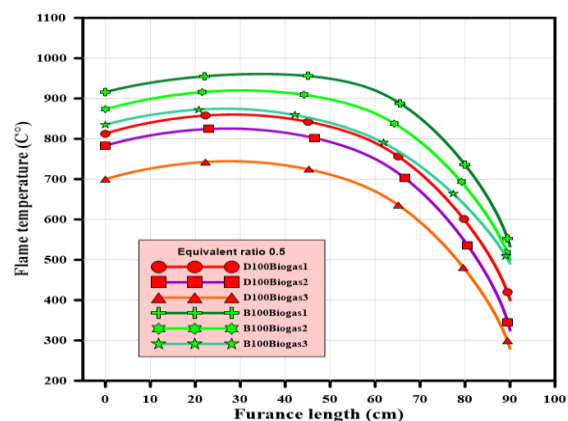


**Figure 8.** The flame temperature at the centerline of a furnace at an equivalence ratio equal to 0.5.

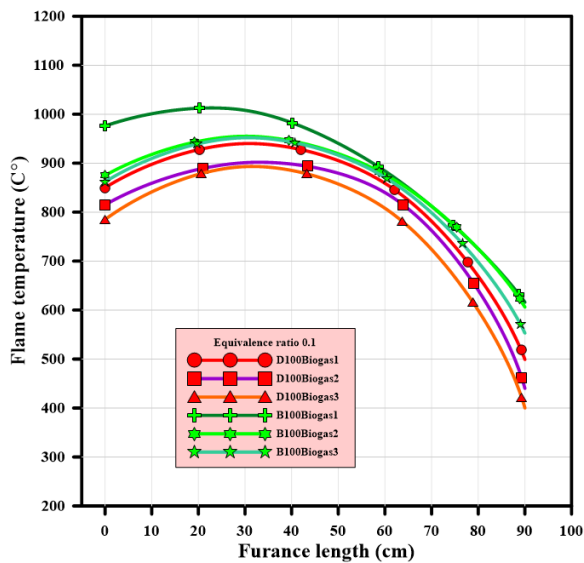


**Figure 9.** The flame temperature at the centerline of a furnace at an equivalence ratio equal to 0.1.

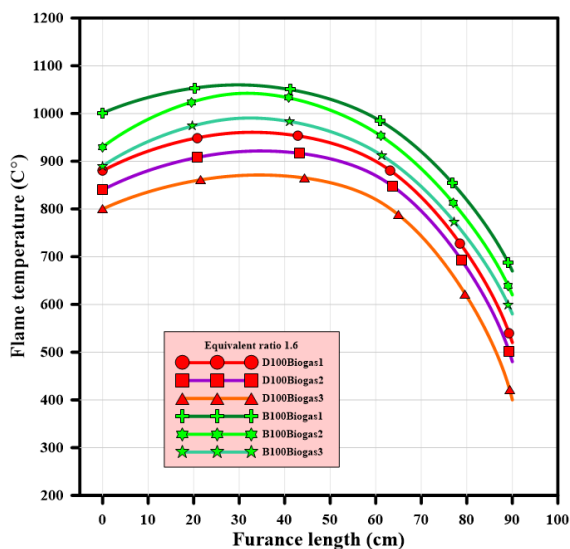


**Figure 10.** The flame temperature at the centerline of a furnace at an equivalence ratio equal to 1.6.

### The effect of different equivalence ratios on the flame pictures and flame contour

Figures 11,12 and 13 display flame contours and flame pictures for test fuels at different equivalence ratios. Digital cameras were used to capture these images. temperature contours for flames with various fuel mixtures conclude from thermocouples measurement installed at four axial and four transverse planes within the furnace, there are discernible changes in the thermal structure for four cases of tested fuels.

It is noticeable that the equivalent ratio has an important effect on the flame that can be controlled by the air supply. We note from the figures that in the case of co-combustion of biodiesel and biogas, the fuel mixtures B100biogas1 and B100biogas3 have a reaction zone including a significant region of high

flame temperature in comparison to D100biogas1 and D100biogas3 for all equivalent ratios.

This is because biodiesel burns more efficiently due to the presence of double bonds in its chemical structure and its high oxygen content concentration. additionally, as the equivalence ratio increases, the flame temperature increase, and the flame area expanded due to adding an excess amount of fuel.

In all cases, the inert carbon dioxide gas had a significant effect on the flame structure and brightness, indicating a slowing of the oxidation reaction and combustion rate, which would lower the flame temperature due to the carbon dioxide dilution effect. Figures 11 and 12 show temperature contour plots at an equivalence ratio of 0.5 for the tested fuels to describe the tested fuel and determine the location of the reaction zone inside the flame.

We note a significant decrease in the temperature distribution inside the furnace as a result of the high percentage of carbon dioxide in the biogas, which is due to the effect of inert gas dilution on the combustion reactions and the flame temperature.

The findings indicate that the maximum flame temperatures of the fuels B100biogas1 and D100biogas1 were about 960 °C and 860 °C, respectively. By increasing the CO<sub>2</sub> ratio in the biogas composition for B100biogas1 and D100biogas1, the maximum temperature inside the furnace is reduced by 9% and 14%, respectively. For all test fuels, the hotter reaction zone occurs at a distance of 0.3 to 0.4 from the burner.

Visually, the yellow luminosity decreased as the inert carbon dioxide ratio increased, and the flame has become unstabilized within the furnace, especially for case D100biogas3. Thus, it is recommended to reduce the CO<sub>2</sub> percentage in biogas to 30% or less.

In the case of D100biogas1 and B100biogas1, the flame exhibits direct brilliance dramatically, and transparency. Due to complete combustion. With a rising equivalence ratio, flame brightness increases dramatically. In the case of D100biogas3 and B100biogas3, on the other hand, according to temperature measurements, the structure of the flames shows a decline in flame size and temperature levels as the amount of CO<sub>2</sub> in biogas composition increases. the formation of a weak and unstable flame.

A low heat zone is also included This is to be expected in flames with lower heating values. The 40% CO<sub>2</sub> flame also exhibits extremely low-temperature values and the formation of a weak and unstable flame. A low heat zone is also included. Mansour et al. (2020).

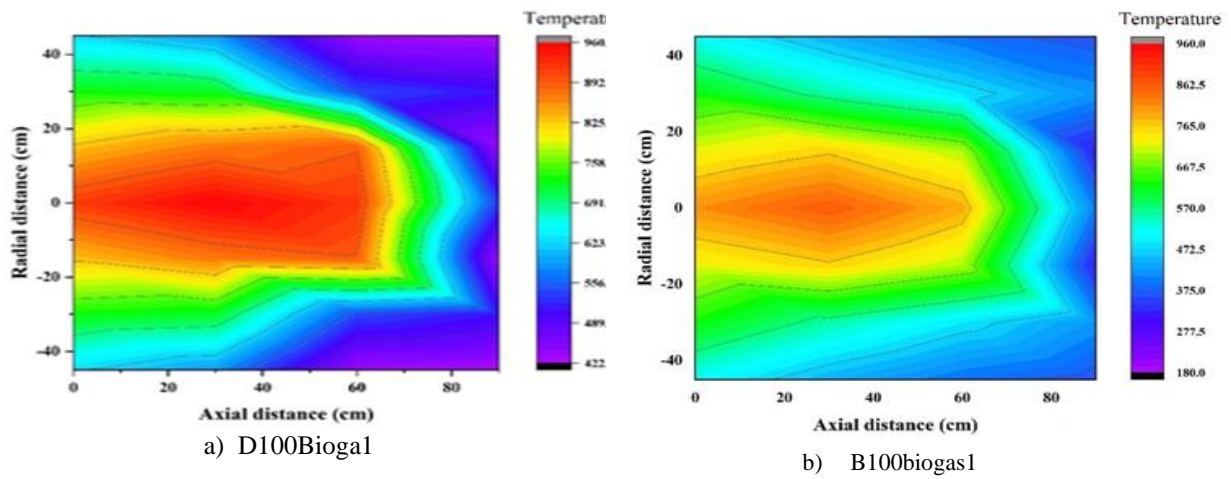


Figure 11. Temperature contour plots of (a) D100Bioga1 and (b) B100Bioga1 at an equivalent ratio of 0.5

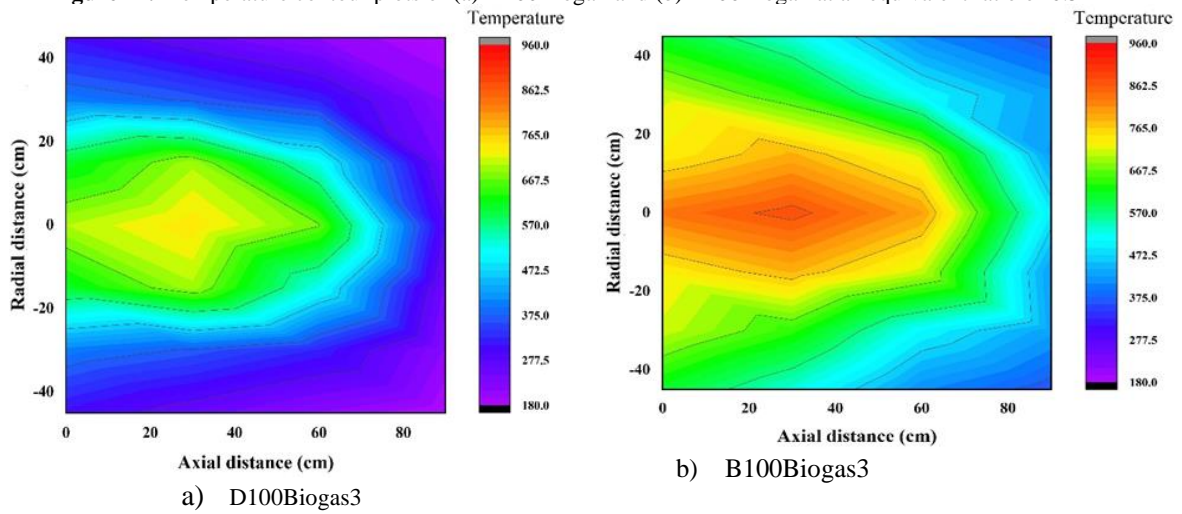


Figure 12. Temperature contour plots of (a) D100Bioga3 and (b) B100Bioga3 at an equivalent ratio of 0.5

Fuels	Equivalence ratio		
	0.5	1	1.6
D100biogas1			
D100biogas3			
B100biogas1			
B100biogas3			

Figure 13. The images of flames of different fuels at various equivalent ratios.

## Conclusion

The experiments are performed to investigate the combustion performance and emission characteristics of different ratios of biogas co-firing with diesel or biodiesel in a 350-kW industrial swirl burner. All types of fuels were tested under similar operating conditions with varying equivalency ratios, and all fuel comparative data was analyzed.

The ratio of CO<sub>2</sub> in the composition of biogas impacts the creation of the product and plays a key role in the chemical reaction. As a result, it affects flame temperature, NO<sub>x</sub> emissions, and CO emissions; in general, as the CO<sub>2</sub> ratio in the biogas composition increases, the flame becomes unstable, NO<sub>x</sub> and temperature decrease, and CO emissions increase.

The co-combustion of biogas with biodiesel (B100biogas1, B100biogas2, and B100biogas3) results in a significant reduction in CO emissions by 60%, 50%, and 42%, respectively, and significant increases in NO<sub>x</sub> emissions by 52%, 47%, and 43%, respectively, compared to conventional diesel.

The maximum flame temperature at roughly 0.3 to 0.4 m from the burner and the exhaust flame temperature increase when the biogas co-combusts with biodiesel than diesel. The co-combustion of biogas with biodiesel (B100biogas1, B100biogas2, and B100biogas3) significantly increases maximum temperature by 10%, 11%, and 12%, respectively, and increases exhaust temperature by 12%, 9%, and 7%, respectively, compared to the co-combustion of diesel with biogas.

The area and intensity of the flame increased in the case of co-combustion of biogas with biodiesel compared to diesel, as well as the intensity and brightness of the flame.

In general, biogas and biodiesel co-combustion produced the highest-intensity flame with the best flame stability. Furthermore, the lowest emission level.

It has been found that in practical experiments, the use of biogas co-combustion with diesel or biodiesel has a positive effect on the combustion performance and emissions in the industrial burner, in addition to reducing the burden of disposing of waste cooking oil and biogas resulting from anaerobic digestion of wastewater treatment by using it as a source of energy and benefiting from it in industrial applications.

We recommend conducting a future study on the effect of adding hydrogen to biogas, which has a carbon dioxide ratio exceeding 30% in co-combustion with diesel or biodiesel, in terms of enhancing flame stability.

## Reference

- Adam AA, A Shahein M, A Moneib HJERJ (2022) Overall Assessment of an Innovative Coaxial Air-Staged Burner for Cofiring of Oil and Gas 173:316-331
- Agwu O, Runyon J, Goktepe B, Chong CT, Ng J-H, Giles A, Valera-Medina A (2020) Visualisation and performance evaluation of biodiesel/methane co-combustion in a swirl-stabilised gas turbine combustor. *Fuel* 277:118172
- Agwu O, Valera-Medina A (2020) Diesel/syngas co-combustion in a swirl-stabilised gas turbine combustor. *International Journal of Thermofluids* 3-4:100026
- Alagu K, Venu H, Jayaraman J, Raju VD, Subramani L, Appavu P, S D (2019) Novel water hyacinth biodiesel as a potential alternative fuel for existing unmodified diesel engine: Performance, combustion and emission characteristics. *Energy* 179:295-305
- Altaher MA, Li H, Andrews GE (2012) Co-Firing of Kerosene and Biodiesel With Natural Gas in a Low NO<sub>x</sub> Radial Swirl Combustor. *ASME Turbo Expo 2012: Turbine Technical Conference and Exposition*, pp 557-567
- Amirnordin SH, Ihsanulhadi N, Alimin AJ, Khalid A (2013) Effects of Palm Oil Biodiesel Blends on the Emissions of Oil Burner. *Applied Mechanics and Materials* 315:956-959
- Balat M (2007) Production of Biodiesel from Vegetable Oils: A Survey. *Energy Sources, Part A: Recovery, Utilization, and Environmental Effects* 29:895-913
- Balat M, Balat H (2009) Biogas as a Renewable Energy Source—A Review. *Energy Sources, Part A: Recovery, Utilization, and Environmental Effects* 31:1280-1293
- Ban-Weiss GA, Chen JY, Buchholz BA, Dibble RW (2007) A numerical investigation into the anomalous slight NO<sub>x</sub> increase when burning biodiesel; A new (old) theory. *Fuel Processing Technology* 88:659-667
- Bazooyar B, Shariati A, Hashemabadi SH (2015) Characterization and Reduction of NO during the Combustion of Biodiesel in a Semi-industrial Boiler. *Energy & Fuels* 29:6804-6814.

- Chen W-H, Liao C-Y, Hung C-I, Huang W-L (2012) Experimental study on thermoelectric modules for power generation at various operating conditions. *Energy* 45:874-881
- Chong CT, Chiong M-C, Ng J-H, Tran M-V, Valera-Medina A, Józsa V, Tian B (2020) Dual-Fuel Operation of Biodiesel and Natural Gas in a Model Gas Turbine Combustor. *Energy & Fuels* 34:3788-3796
- Colorado A, Herrera B, Amell A (2010) Performance of a flameless combustion furnace using biogas and natural gas. *Bioresource technology* 101:2443-2449
- De Mes T, Stams A, Reith J, Zeeman G (2003) Methane production by anaerobic digestion of wastewater and solid wastes. *Bio-methane & Bio-hydrogen*:58-102
- Divya D, Gopinath LR, Merlin Christy P (2015) A review on current aspects and diverse prospects for enhancing biogas production in sustainable means. *Renewable and Sustainable Energy Reviews* 42:690-699
- Elkelawy M, Alm-Eldin Bastawissi H, Esmail KK, Radwan AM, Panchal H, Sadasivuni KK, Ponnamma D, Walvekar R (2019) Experimental studies on the biodiesel production parameters optimization of sunflower and soybean oil mixture and DI engine combustion, performance, and emission analysis fueled with diesel/biodiesel blends. *Fuel* 255:115791
- Elkelawy M, Alm Eldin Mohamad H, Abdel-Rahman AK, Abou Elyazied A, Mostafa El malla S (2022a) Biodiesel as an Alternative Fuel in Terms of Production, Emission, Combustion Characteristics for Industrial Burners: a Review %J *Journal of Engineering Research* 6:45-52
- Elkelawy M, Bastawissi HA-E, Esmail KK, Radwan AM, Panchal H, Sadasivuni KK, Suresh M, Israr M (2020) Maximization of biodiesel production from sunflower and soybean oils and prediction of diesel engine performance and emission characteristics through response surface methodology. *Fuel* 266:117072
- Elkelawy M, El Shenawy EA, Bastawissi HAE, El Shennawy IA (2022b) The effect of using the WCO biodiesel as an alternative fuel in compression ignition diesel engine on performance and emissions characteristics. *Journal of Physics: Conference Series* 2299:012023
- Gad MS, Mahfouz A, Emara A (2021) Spray and combustion characteristics for light diesel/waste cooking oils blended with fuel additives inside an industrial boiler. *Fuel* 286:119247
- Hosseini SB, Bashirnezhad K, Moghiman A, Khazraii Y, Nikoofal NJP (2010) Experimental comparison of combustion characteristic and pollutant emission of gas oil and biodiesel 220:60Hz
- Hosseini SE, Abdul Wahid M (2015) Effects of Burner Configuration on the Characteristics of Biogas Flameless Combustion. *Combustion Science and Technology* 187:1240-1262
- Issariyakul T, Kulkarni MG, Dalai AK, Bakhshi NN (2007) Production of biodiesel from waste fryer grease using mixed methanol/ethanol system. *Fuel Processing Technology* 88:429-436
- Janakiraman S, Lakshmanan T, Chandran V, Subramani L (2020) Comparative behavior of various nano additives in a DIESEL engine powered by novel *Garcinia gummi-gutta* biodiesel. *Journal of Cleaner Production* 245:118940
- Jiang L (2014) Investigation of atomization mechanisms and flame structure of a twin-fluid injector for different liquid fuels. *The University of Alabama, Ann Arbor*, p 207.
- Kapoor R, Ghosh P, Tyagi B, Vijay VK, Vijay V, Thakur IS, Kamyab H, Nguyen DD, Kumar A (2020) Advances in biogas valorization and utilization systems: A comprehensive review. *Journal of Cleaner Production* 273:123052
- KIPYEGON BI (2011) BIOGAS USE IN POWER GENERATION. University of Nairobi
- Kumar Yadav V, Ray A, Ravi MR (2019) Experimental and computational investigation of the laminar burning velocity of hydrogen-enriched biogas. *Fuel* 235:810-821
- Kumaran P, Gopinathan M, Kantharajan S (2014) COMBUSTION CHARACTERISTICS OF IMPROVED BIODIESEL IN DIFFUSION BURNER. *International Journal of Automotive and Mechanical Engineering* 10:2112-2121
- Kurji H, Valera-Medina A, Okon A, Chong CT (2017) Combustion and emission performance of CO<sub>2</sub>/CH<sub>4</sub>/biodiesel and CO<sub>2</sub>/CH<sub>4</sub>/diesel blends in a Swirl Burner Generator. *Energy Procedia* 142:154-159

- Lee C-E, Hwang C-H (2007) An experimental study on the flame stability of LFG and LFG-mixed fuels. *Fuel* 86:649-655
- Lee MC, Seo SB, Yoon J, Kim M, Yoon Y (2012) Experimental study on the effect of N<sub>2</sub>, CO<sub>2</sub>, and steam dilution on the combustion performance of H<sub>2</sub> and CO synthetic gas in an industrial gas turbine. *Fuel* 102:431-438
- Leonov ES, Trubaev PA (2021) Analysis of biogas content influence on the flame properties. *IOP Conference Series: Materials Science and Engineering* 1089:012032
- Leung DYC, Guo Y (2006) Transesterification of neat and used frying oil: Optimization for biodiesel production. *Fuel Processing Technology* 87:883-890
- Leung T, Wierzbka I (2008) The effect of hydrogen addition on biogas non-premixed jet flame stability in a co-flowing air stream. *International journal of hydrogen energy* 33:3856-3862
- Liu D, Liu D, Zeng RJ, Angelidaki I (2006) Hydrogen and methane production from household solid waste in the two-stage fermentation process. *Water Research* 40:2230-2236
- Love ND, Jr. (2009) Effects of equivalence ratio and iodine number on nitrogen oxide emissions from the flames of biofuels and hydrocarbons. *The University of Oklahoma, Ann Arbor*, p 303
- Mahfouz A, Emara A, Gad M, El Fatih AJJRASET (2017) Effect of waste cooking-diesel oils blends on performance, emissions and combustion characteristics of industrial oil burner 5:1264-1274
- Mansour MS, Abdallah MS, Allam NK, Ibrahim AM, Khedr AM, Al-Bulqini HM, Zayed MF (2020) Biogas production enhancement using nanocomposites and its combustion characteristics in a concentric flow slot burner. *Experimental Thermal and Fluid Science* 113:110014
- Meng X, Chen G, Wang Y (2008) Biodiesel production from waste cooking oil via alkali catalyst and its engine test. *Fuel Processing Technology* 89:851-857
- Miltner M, Makaruk A, Harasek M (2017) Review on available biogas upgrading technologies and innovations towards advanced solutions. *Journal of Cleaner Production* 161:1329-1337
- Moffat RJ (1988) Describing the uncertainties in experimental results. *Experimental Thermal and Fluid Science* 1:3-17
- Moreno Ovalle F (2017) Combustion Characteristics of Three-component Fuel Blends in a Porous Media Burner at Lean Conditions
- Phan AN, Phan TM (2008) Biodiesel production from waste cooking oils. *Fuel* 87:3490-3496
- Pinto MJpM (2012) Biodiesel fuel formulation. *Universidade de Aveiro (Portugal), Ann Arbor*, p 322
- Pourhoseini SH, Namvar-Mahboub M, Hosseini E, Alimoradi A (2021) A comparative exploration of thermal, radiative and pollutant emission characteristics of oil burner flame using palm oil biodiesel-diesel blend fuel and diesel fuel. *Energy* 217:119338
- Queirós P, Costa M, Carvalho RH (2013) Co-combustion of crude glycerin with natural gas and hydrogen. *Proceedings of the Combustion Institute* 34:2759-2767
- Raju VD, Venu H, Subramani L, Kishore PS, Prasanna PL, Kumar DV (2020) An experimental assessment of prospective oxygenated additives on the diverse characteristics of diesel engine powered with waste tamarind biodiesel. *Energy* 203:117821
- Rashid U, Anwar F, Moser BR, Ashraf S (2008) Production of sunflower oil methyl esters by optimized alkali-catalyzed methanolysis. *Biomass and Bioenergy* 32:1202-1205
- Ratel G, Michotte C, Bochud FO (2015) Uncertainty of combined activity estimations. *Metrologia* 52:S30-S41
- Sidey J, Mastorakos E (2017) Visualisation of turbulent swirling dual-fuel flames. *Proceedings of the Combustion Institute* 36:1721-1727
- Sidey JAM, Mastorakos E (2018) Stabilisation of swirling dual-fuel flames. *Experimental Thermal and Fluid Science* 95:65-72
- Subramani L, Venu H (2019) Evaluation of methyl ester derived from novel *Chlorella emersonii* as an alternative feedstock for DI diesel engine & its combustion, performance and tailpipe emissions. *Heat and Mass Transfer* 55:1513-1534.

- Swamy DLSVN, Kowsik Y, Dhana Raju V, Appa Rao K, Venu H, Subramani L, Bala Prasad K (2019) Effect of 1-butanol on the characteristics of diesel engine powered with novel tamarind biodiesel for the future sustainable energy source. *Energy Sources, Part A: Recovery, Utilization, and Environmental Effects*:1-19
- Talebian-Kiakalaieh A, Amin NAS, Mazaheri H (2013) A review on novel processes of biodiesel production from waste cooking oil. *Applied Energy* 104:683-710
- Tashtoush G, Al-Widyan MI, Al-Shyoukh AO (2003) Combustion performance and emissions of ethyl ester of a waste vegetable oil in a water-cooled furnace. *Applied Thermal Engineering* 23:285-293
- Topare NS, Jogdand RI, Shinde HP, More RS, Khan A, Asiri AM (2022) A short review on approach for biodiesel production: Feedstock's, properties, process parameters and environmental sustainability. *Materials Today: Proceedings* 57:1605-1612.
- Venu H, Raju VD, Subramani L (2019a) Influence of injection timing on torroidal re-entrant chamber design in a single cylinder DI engine fuelled with ternary blends. *Heat and Mass Transfer* 55:2931-2948
- Venu H, Raju VD, Subramani L, Appavu P (2020) Experimental assessment on the regulated and unregulated emissions of DI diesel engine fuelled with *Chlorella emersonii* methyl ester (CEME). *Renewable Energy* 151:88-102
- Venu H, Subramani L, Raju VD (2019b) Emission reduction in a DI diesel engine using exhaust gas recirculation (EGR) of palm biodiesel blended with TiO<sub>2</sub> nano additives. *Renewable Energy* 140:245-263
- Weiland P (2010) Biogas production: current state and perspectives. *Applied microbiology and biotechnology* 85:849-860
- Zhang L, Hui S, Yang Y, Sun R, Ismail TM, Abd El-Salam M, Ren X (2019) Numerical and Experimental Assessment of a Novel Multinozzle Burner with CO<sub>2</sub> Diluent to Improve the Emissions from a Swirling Flame in a Combustion Chamber. *Energy & Fuels* 33:7869-7885
- Zhang Y, Dubé MA, McLean DD, Kates M (2003) Biodiesel production from waste cooking oil: 1. Process design and technological assessment. *Bioresource Technology* 89:1-16
- Zhen H, Leung C, Cheung C (2013) Effects of hydrogen addition on the characteristics of a biogas diffusion flame. *International journal of hydrogen energy* 38:6874-6881.